NANO LETTERS

pubs.acs.org/NanoLett

Mini Review

Lithium-Conducting Branched Polymers: New Paradigm of Solid-State Electrolytes for Batteries

Shu-Meng Hao, Shuang Liang, Christopher D. Sewell, Zili Li, Caizhen Zhu,* Jian Xu, and Zhiqun Lin*

Cite This: *Nano Lett.* 2021, 21, 7435−7447

Read Online

ACCESS | Metrics & More | Article Recommendations

ABSTRACT: The past decades have witnessed rapid development of lithium-based batteries. Significant research efforts have been progressively diverted from electrodes to electrolytes, particularly polymer electrolytes (PEs), to tackle the safety concern and promote the energy storage capability of batteries. To further increase the ionic conductivity of PEs, various branched polymers (BPs) have been rationally designed and synthesized. Compared with linear polymers, branched architectures effectively increase polymer segmental mobility, restrain crystallization, and reduce chain entanglement, thereby rendering BPs with greatly enhanced lithium transport. In this Mini Review, a diversity of BPs for PEs is summarized by scrutinizing their unique topologies and properties. Subsequently, the design principles for enhancing the physical properties, mechanical properties, and electrochemical performance of BP-based PEs (BP-PEs) are provided in which the ionic conduction is particularly examined in light of the Li^+ transport mechanism. Finally, the challenges and future prospects of BP-PEs in this rapidly evolving field are outlined.

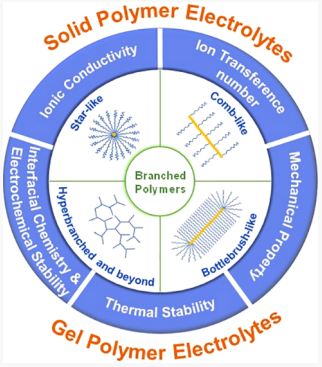

KEYWORDS: *branched polymers, polymer electrolytes, topological structure, lithium-based batteries, ionic conductivity*

1. INTRODUCTION

Ever-increasing demand derived from the extremely rapid development of portable electronic and grid-scale energy storage have entailed continuous exploration of next-generation secondary batteries, among which advanced lithium-based batteries (e.g., lithium−sulfur and lithium−metal batteries) have garnered much attention. Therefore, the development of electrolytes for transporting lithium (i.e., lithium-conducting electrolytes) is of key importance. Notably, conventional liquid electrolytes suffer from several issues such as toxicity, volatility, and flammability. Moreover, liquid electrolytes have inferior antioxidation abilities at high voltages. To this end, replacing liquid electrolytes with lithium-conducting polymer electrolytes (PEs) has been widely recognized as a promising route to alleviating the concerns noted above. PEs are solid-state electrolytes (SSEs) with polymer frameworks, including solid polymer electrolytes (SPEs) and gel polymer electrolytes (GPEs). The flexibility, stretchability, and mechanical strength impart PEs with good processability, intimate contact with electrodes, and the ability to suppress lithium dendrite.[1−3] Additionally, the development of PEs also afford a promising prospect for assembling flexible devices. However, PEs, particularly SPEs, encounter unsatisfactory ionic conductivity with nonuniform ion distribution. The trade-off between ionic conductivity and mechanical property also imposes a challenge for PEs to concurrently reach high ionic conductivity and mechanical robustness, ultimately limiting their practical applications. Moreover, compared with solid ceramic electrolytes, the dual-ion transport in traditional PEs results in an inferior Li^+ transference number, which decreases the charge transport efficiency and could in turn accelerate the formation of lithium dendrite. Additionally, relatively higher electrode−electrolyte interfacial resistance of PEs than that of liquid electrolytes could further impair the battery performance.

Among all the challenges that PEs face, the inferior ionic conductivity of PEs than that of liquid electrolytes manifests a significant obstacle to high electrochemical performance. Therefore, the ability to increase ionic conductivity of PEs represents an important endeavor. An electrolyte conductivity can be calculated by the following equation[4]

$$\sigma = \sum p_i q_i \mu_i \tag{1}$$

where p_i, q_i, and μ_i are the concentration of free ions, charge of ions, and mobility of ions, respectively, for the ion species i, and the ionic conductivity equals the sum of all the ion species in the electrolyte. The ion mobility can be calculated according to the Einstein relation[4]

$$\mu_i = q_i D_i/(k_B T) \tag{2}$$

Received: July 19, 2021
Published: September 13, 2021

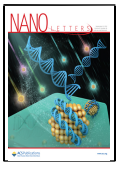

https://doi.org/10.1021/acs.nanolett.1c02558
Nano Lett. 2021, 21, 7435−7447

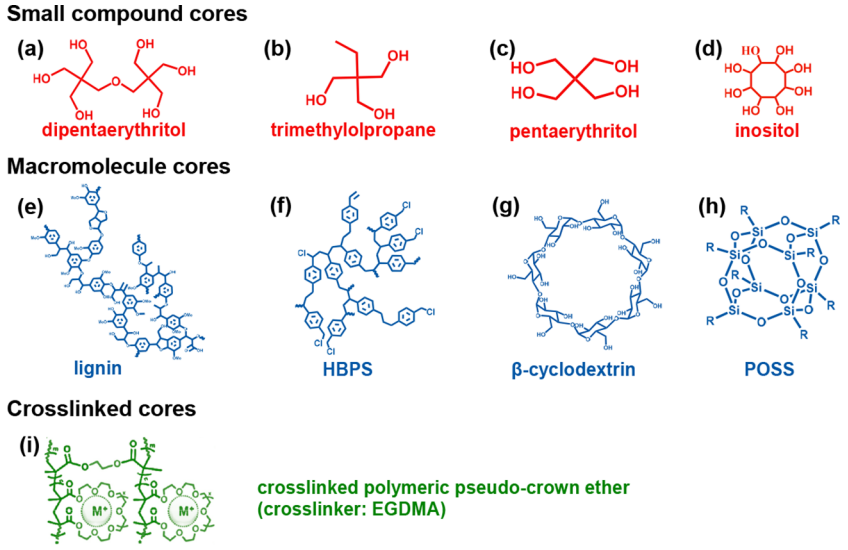

Figure 1. Chemical structures of (a–d) small compounds, (e–h) macromolecules, and (i) cross-linked cores for SP-PEs. (i) Reproduced from ref 16 with permission. Copyright 2019 Elsevier B.V.

where D, k_B, and T signify the diffusion coefficient, Boltzmann constant, and temperature, respectively. Combining eqs 1 and 2, an electrolyte conductivity is dominated by the concentration of free ions, diffusion coefficient, and charge of ions. For electrolytes with highly soluble salts, the ion diffusion is the determining factor for high ionic conductivity. On the basis of the Stokes–Einstein relation, diffusion coefficient is inversely proportional to viscosity (η) at low Reynolds numbers: $D = k_BT/(6\pi\eta r_i)$ (r_i: ion radius).[4] The Maxwell model reveals $\eta = G\tau_s$ in which G and τ_s are glassy modulus and structural relaxation time, respectively.[4] As a result, diffusion coefficient is dependent on viscosity and structural relaxation time: $D \propto T/\eta \propto T/\tau_s$. For polymers, the relaxation time is highly related to the local segmental dynamics, and viscosity is controlled by the motion of the entire chain.[4]

Therefore, incorporating polymers with high chain mobility is essential to increasing the ionic conductivity of PEs. In this context, polymers should possess a low glass-transition temperature (T_g), restrained crystallinity, and low degrees of chain entanglement.[5] Nevertheless, conventional linear polymers used in PEs are semicrystalline, which drastically limits the area that can effectively transport Li^+. The high T_g and large degree of chain entanglement due to long polymer chain required to provide sufficient mechanical robustness further suppress the chain motion and subsequent ionic conduction. Taking linear poly(ethylene oxide) (PEO) as an example, although it favors lithium desolvation from lithium salt as well as provides ample ether groups to coordinate with Li^+, pure linear PEO suffers from inferior ionic conductivity ($\sigma = 10^{-6}$–10^{-8} S cm^{-1}) at room temperature (RT), thus greatly restricting its electrochemical performance. Fortunately, polymer chain dynamics can be tuned by constructing branched architecture. At the same molecular weight (MW), branched polymers (BPs) have shorter chains than linear analogues, making chains more difficult to fold into an ordered structure. More importantly, the core or backbone of BPs can function as inherent defects, which tend to migrate to the surface of crystals, rather than being included in the crystal lattice.[6] As a result, the crystallization of polymers can be completely restrained with sufficient branches, leading to a purely amorphous state. The shorter chains and unique topologies of BPs (e.g., radiating architecture) can also reduce chain entanglement, thereby decreasing the polymer viscosity.[7] Additionally, BPs possess numerous chain ends, which can not only be functionalized (e.g., serving as cross-linking active sites, introducing polar groups, and so forth) by replacing end groups but also increase BP segmental mobility due to their dangling feature and conformational freedom, thereby decreasing T_g of BP.[8] Moreover, some unique topologies render BPs special properties such as high solubility in common solvents, controllable self-assembling structures, and tunable thermal properties. Thus, crafting BPs with rationally designed topologies stands out as an effective route to improving chain mobility and constructing high-performance PEs.

Inspired by the appealing attributes of PEs as noted above, the past decade has been witness to many reviews discussing the properties of PEs and their implementation in PE-based batteries.[9,10] However, all of these reviews have concentrated on the composition design of linear polymers. Yet, the rapid development of BPs for PEs has been either largely overlooked or discussed in a considerably limited scope. In the latter context, the topologies of BPs, as well as the architecture effects and design strategies for enhancing the properties and electrochemical performance of branched-polymer-based PEs (BP-PEs), have not been comprehensively summarized. Notably, progress in living free-radical polymerization techniques and design strategies have afforded access to a rich variety of topologically intriguing BPs, manifesting great potential as lithium-conducting polymers for PEs. Clearly, there is a vital need to review BP-PEs for batteries. Herein, we comprehensively assess the use of BP-PEs for lithium conducting from the viewpoints of the effects of the BPs of different chain architectures on an array of physical properties, mechanical properties, and electrochemical performance of BP-PEs as well as the design strategies for creating high-performance BP-PEs. First, a variety of BPs, including starlike polymers (SPs), comblike polymers (CPs), bottlebrush-like polymers (BBPs), and hyperbranched polymers (HBPs) are critically discussed and compared in light of their intriguing topologies and properties. Subsequently, design strategies via tailoring the synthesis parameters to yield BP-PEs with

https://doi.org/10.1021/acs.nanolett.1c02558
Nano Lett. 2021, 21, 7435–7447

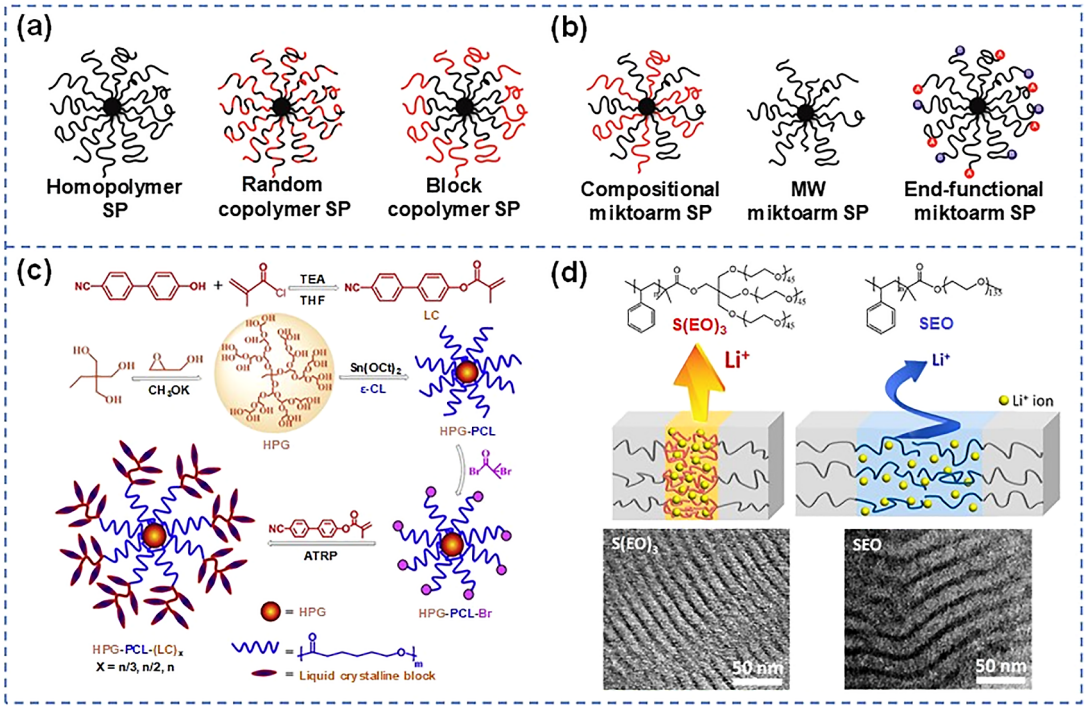

Figure 2. Schematics of SP categories based on (a) composition and sequence distribution of each individual arm and (b) miktoarm species. Reproduced from ref 17 with permission. Copyright 2016 American Chemical Society. (c) Synthetic routes to the SP with liquid crystal $(LC)_x$ on the outer shell. Reproduced from ref 19 with permission. Copyright 2018 Elsevier B.V. (d) Schematic of lithium transport pathways in miktoarm SP ($S(EO)_3$) and linear analogue (SEO), as well as corresponding chemical structures and cross-sectional TEM images of $S(EO)_3$ and SEO (PEO phases were stained by RuO_4). Reproduced from ref 20 with permission. Copyright 2018 American Chemical Society.

enhanced physical properties, mechanical properties, and electrochemical performance are provided, including ionic conductivity, ion transference number, mechanical property, thermal stability, and interfacial chemistry and electrochemical stability. Among them, ionic conductivity based on the mechanism of Li^+ transport is particularly scrutinized, followed by highlighting the means of constructing Li^+ transport channels. Finally, the challenges and opportunities for future development of BP-PEs for high-performing lithium-based batteries are presented.

2. BRANCHED POLYMERS OF DIVERSIFIED TOPOLOGIES FOR POLYMER ELECTROLYTES

2.1. Starlike Polymers (SPs). SPs are branched macromolecule in which more than three linear "arms", composed of homopolymers or copolymers, are tethered to a central branching point (core), forming a spherical architecture. With all the arms anchored on the core, the chains closest to the core tend to be densely packed and stretched; conversely, chains far away from the core have more free space to move. The core of SPs generally contains multiple active reaction sites, and can be categorized into small compounds (e.g., dipentaerythritol, trimethylolpropane, pentaerythritol, inositol),[11,12] macromolecules (e.g., lignin, hyperbranched polystyrene (HBPS), β-cyclodextrin, polyhedral oligomeric silsesquioxane (POSS)),[13−15] and network cores (e.g., cross-linked polymeric pseudocrown ether)[16] (Figure 1).[17] The MW of SPs can be controlled by either increasing the MW of grafted arms or the number of arms connected to the core. Simultaneously, SPs possessing a higher arm number normally require a larger core size than those SPs with limited arm number due to the steric hindrance among arm chains. The core size, arm MW, arm number, and SP MW can all significantly impact the physical and mechanical properties of SPs, especially viscosity and thermal properties, with the most influential factor being situational. When the core size is small and arm number is low, the molecular dynamics and thermal properties are dominated by the arm properties, including arm MW; this occurs due to the low mass fraction of the core which only acts as a branching point in this case.[17] On the contrary, SPs with large cores, such as cross-linked network cores, and high arm numbers resemble core−shell structures; therefore, the impact of the cores are considerable.[17] For rheological properties, besides core microstructure effects, studies have also demonstrated that, while keeping arm MW fixed, higher arm numbers along with larger cores and consequent higher SP MW result in an increased polymer viscosity, potentially changing the polymer solution from Newtonian to viscoelastic behavior.[18]

On the basis of the composition and sequence distribution of each individual arm, SPs can be classified into homopolymers, random copolymers, and block copolymers (Figure 2a).[17] In early studies, starlike topology was only constructed to suppress crystallization and promote the ionic conductivity of polymers, so arms were normally constructed from ether or ester homopolymers such as PEO or poly(poly(ethylene glycol) methyl ether methacrylate) (PPEGMA). Later on, to further increase the ionic conductivity of SPs and concurrently tune other polymer properties, copolymer-type arms were incorporated in SPs. For example, polymers with high T_g, such as polystyrene (PS) and poly(methyl methacrylate) (PMMA), or polymers with cross-linking active sites are integrated in SP arms to enhance the mechanical robustness and thermal stability.[13] Additionally, using liquid-crystal-containing copoly-

https://doi.org/10.1021/acs.nanolett.1c02558
Nano Lett. 2021, 21, 7435−7447

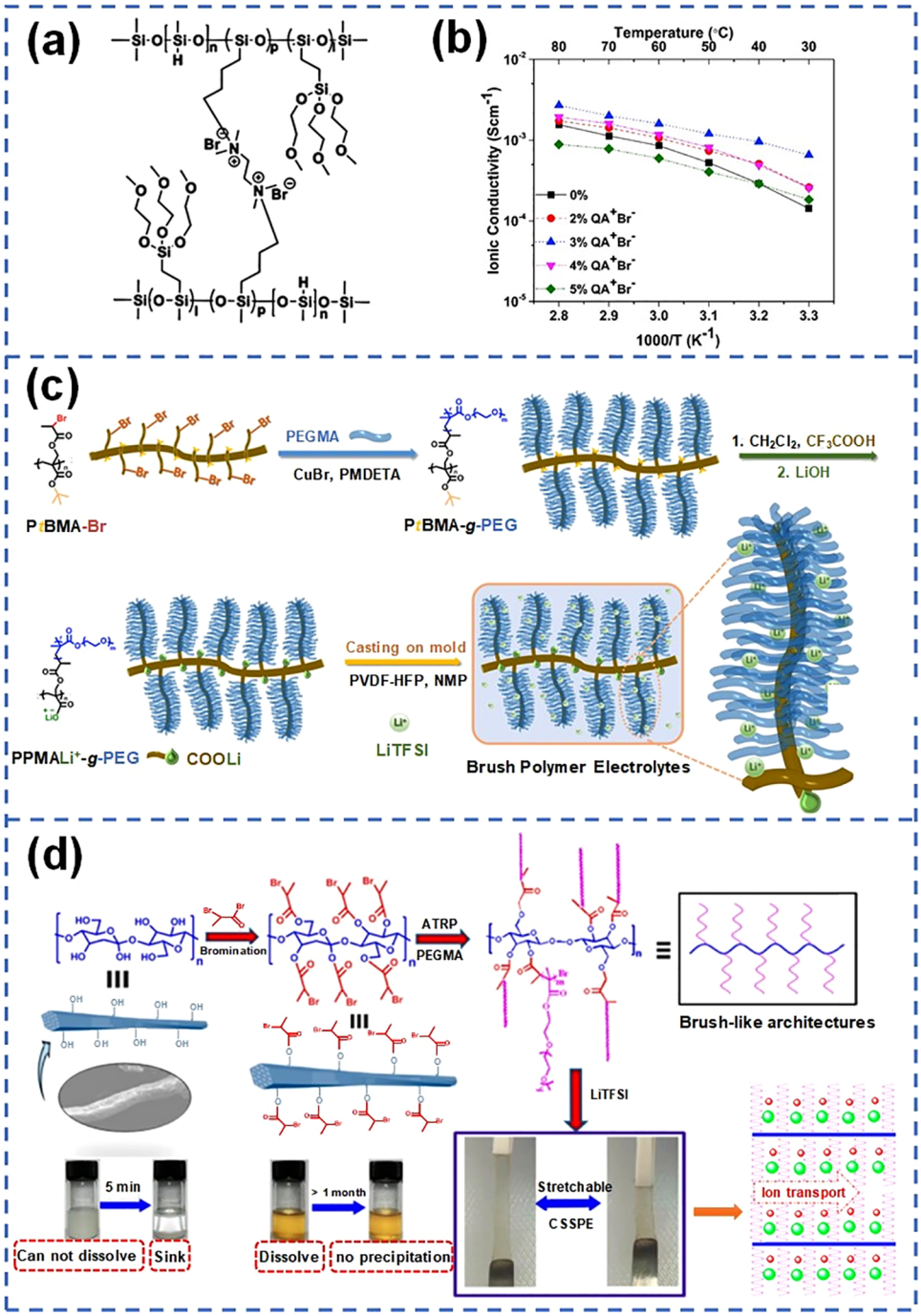

Figure 3. (a) Chemical structure of synthesized comb-like quaternized-ammonium brominated poly(methylhydrosiloxane) (QA^+Br^-). (b) Temperature-variable ionic conductivities of polysiloxane SPEs with different cross-linking ratios. Reproduced from ref 25 with permission. Copyright 2020 Elsevier B.V. (c) Synthetic route to bottlebrush-like PPMALi-*g*-PEG. Reproduced from ref 28 with permission. Copyright 2019 American Chemical Society. (d) Synthetic route to cellulose-based BBPs with PPEGMA brushes. Reproduced from ref 29 with permission. Copyright 2019 American Chemical Society.

mer arms in SPs to construct ion diffusion channels has attracted extensive attention (Figure 2c).[19] Owing to the orientation of liquid crystal, ion diffusion channels could be constructed that effectively transport Li^+.

Miktoarm SPs are another notable kind of macromolecule for PEs in which the polymer arms anchored onto the core vary from each other in some way, such as differing compositions, functionalities, and/or MWs (Figure 2b). Miktoarm SPs possess different properties from the above-mentioned starlike copolymers and linear copolymers, especially after self-assembly. Up until now, only limited studies regarding the application of miktoarm SPs in PEs have been reported. Park and co-workers synthesized a miktoarm starlike copolymer ($S(EO)_3$) in which three PEO arms and one PS chain were connected by a pentaerythritol tribromide core.[20] Miktoarm $S(EO)_3$, in comparison to the analogous linear S(EO) of equal MW, presented a similar lamellar morphology but decreased thicknesses of the PS and PEO

https://doi.org/10.1021/acs.nanolett.1c02558
Nano Lett. 2021, 21, 7435−7447

domains (Figure 2d). The PEO phase had a smaller volume fraction in miktoarm $S(EO)_3$ than in linear SEO, making the Li^+ effectively concentrated in PEO phase and facilitating Li^+ transport. As a result, the miktoarm starlike $S(EO)_3$ exhibited a good RT ionic conductivity of $\sim 10^{-5}$ S cm^{-1}, outperforming the linear analogue SEO.

2.2. Comblike Polymers (CPs). CPs are a kind of BP in which monomers, oligomers, or macromonomers are anchored onto polymeric backbones with the aid of various chemical junctions. These polymeric backbones generally have a linear structure, and the grafted molecular chains, referred as side chains, dangle along the backbone.[23] Compared with linear polymers, comb-like topologies can restrict polymer crystallization to some extent, but the orderly packing of CP side chains could still occur at relatively low grafting density and high side chain MW. Despite the dominating effect of side chains on CP crystallization, the properties and compositions of the linear backbone, such as conformational rigidity, also impact the polymer thermal properties. For example, a CP with rigid polymer backbone (poly(p-benzamide), PBA) showed lower crystallinity than one with flexible polymer backbone (poly(ethylenimine), PEI).[24] Additionally, the backbone of CPs can offer a confined environment in which the side chains display thermodynamic and crystallization behaviors that differ from the linear analogues.[23] CPs can be synthesized by directly polymerizing macromonomers (grafting-through route) in which case the backbones are derived from the involved macromonomers. Furthermore, the pendant side chains can also grow from (grafting-from route), or be grafted to (grafting-to route), the existing backbones (e.g., poly(methylhydrogensiloxane) (PMHS), poly(ethylene-altmaleic) anhydride (PEaMA)).[25,26]

CPs with polysiloxane backbones and lithium-conducting side chains have attracted much attention over the past decades. Polysiloxanes have abundant Si−O−Si bonds, which possess a low bond rotation barrier (0.8 kJ mol^{-1}) and high flexibility, endowing polysiloxane-based CPs with potential for fast ion transport. In 1986, polysiloxane-based CPs with PEO side chains were first reported, displaying a high ionic conductivity of $\sim 10^{-4}$ S cm^{-1}.[27] However, the Si−O−C branched side chains suffered from poor chemical stability.[27] This issue was later addressed by switching the branching sites from Si−O−C to Si−C, laying the foundation for the future development of polysiloxane-based CP-PEs. Polysiloxane-based CP-PEs can be endowed with outstanding performance by anchoring side chains with different functions on the linear polysiloxane backbone. For example, polysiloxane-based CPs with polyether side chains were functionalized by varying amounts of quaternary ammonium groups.[25] The polar quaternary ammonium groups not only served as cross-linking sites to provide the mechanical robustness (Figure 3a) but also increased the dielectric constant of the SPEs when using the optimal content (~3%), which enhanced the dissociation of lithium and subsequently ion transport. The as-prepared CP-SPEs exhibited an impressive ionic conductivity of 6.6×10^{-4} S cm^{-1} at 30 °C (Figure 3b).

2.3. Bottlebrush-like Polymers (BBPs). BBPs are an important class of BP with high MW. Technically, BBPs are also CPs but with a significantly higher grafting density of the side chains.[34] Each repeating unit of the linear polymeric backbone is attached to one or more polymer side chains (brushes), forming a macromolecular bottlebrush-like structure. Because of the steric repulsion between the densely grafted brushes, BBPs exhibit cylindrical architecture with lower elastic modulus and absent of entanglement.[34] Compared with CPs of which the side chains can physically overlap with an unperturbed random Gaussian conformation, the brushes in BBPs are stretched, segregated, and weakly penetrated.[34] The lack of chain entanglement reduces the energy barriers to reorganization, thereby enabling brushes to serve as "building blocks" for more complex molecular architectures, and to construct ion diffusion pathways.[35] Furthermore, the stretched brushes and high-density branching sites can restrain crystal growth. Besides, the densely grafted brushes lead to the dilution of backbone, rendering BBPs special viscoelastic and mechanical properties, such as ultralow modulus plateau in the soft gel range when the backbones are long.[36] BBPs have been demonstrated to be excellent ion conductors with concentrated charge carriers and fast ion diffusion pathways.[37]

Despite the structural advantages, BBPs in PEs for lithium-based batteries has been rarely reported.[28,38] Recently, a well-defined BBP with short grafted PEO brushes was crafted (Figure 3c).[28] The densely packed and stretched PEO chains facilitate the intrachain and interchain ion hopping, providing channels for ion transport, and thus the polymer exhibited a good ionic conductivity. Additionally, the exposed $-CO_2^-$ groups on the backbone could coordinate with Li^+ to construct single-ion conductors, rendering the BBP-SPE a promoted ion transference number. The BBP-PEs were also reported by using cellulose as backbones and PPEGMA as brushes (Figure 3d).[29] The resulting SPE presented a stretchability over 150%, and an ionic conductivity of 8.00×10^{-5} S cm^{-1} at 30 °C attributed from the constructed ion channels.

2.4. Hyperbranched Polymers (HBPs). HBPs signify the macromolecules with dense branching sites and great number of functional groups. The dendritic, linear, and terminal units randomly distribute along the polymeric backbone, forming a divergent three-dimensional structure.[41] Broadly, dendrimers, as well as some SPs, CPs, and BBPs, can also be classified as HBPs. Therefore, in this context HBPs only refer to highly branched macromolecules without well-defined morphologies and architectures. The irregular three-dimensional HBPs are regarded as low or no chain entanglement, resulting in restrained crystallization, low T_g, outstanding chain mobility, and good processability. Hyperbranching PEO with polar glycerol as branching sites was proven to effectively prevent the SPE crystallization when doped with Li salts, exhibiting 2−3 orders of magnitude higher ionic conductivity than linear analogue below 50 °C.[42] Moreover, because HBPs possessed numerous terminal groups, the ionic conductivity of hyperbranched PEO could be further elevated by replacing the terminal hydroxyl groups to permethylation, indicating the important impacts of terminal groups on HBP properties.[42]

3. PHYSICAL PROPERTIES, MECHANICAL PROPERTIES, AND ELECTROCHEMICAL PERFORMANCE OF BRANCHED POLYMERS FOR POLYMER ELECTROLYTES

3.1. Ionic Conductivity. *3.1.1. Influencing Factors of Lithium Transport in BP-PEs.* Lithium transport in ion-conducting polymers follows a well-known mechanism: Li^+ is first dissociated from lithium salt, followed by coordination with the electron donors (e.g., −O−, ═O, C═O, and −CN) in polymer chains. Polymer chains undergo constant local

https://doi.org/10.1021/acs.nanolett.1c02558
Nano Lett. 2021, 21, 7435−7447

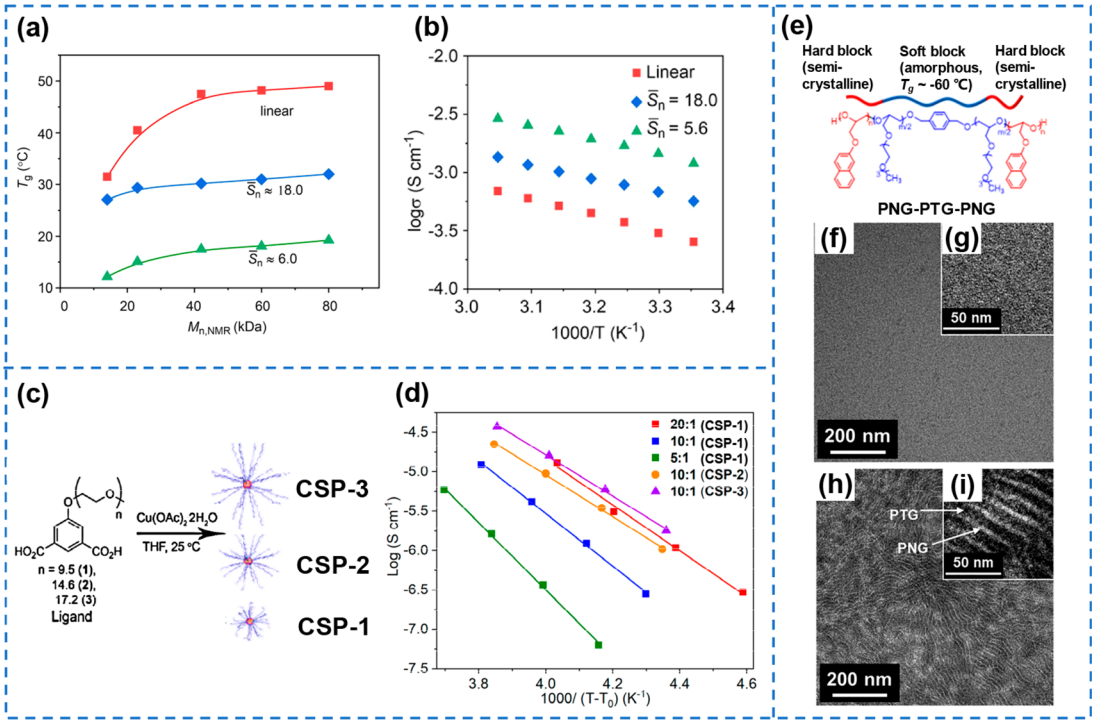

Figure 4. (a) MW-dependent T_g and (b) temperature-dependent ionic conductivities of linear and branched fluoropolymers ($\bar{S}_n$ represents the average number of monomers inserted between two adjacent junctions, evaluating the degree of branching). Reproduced from ref 43 with permission. Copyright 2020 Wiley-VCH. (c) Schematic of the synthesis of CSPs with different arm length, and (d) the corresponding temperature-dependent ionic conductivities (20:1, 10:1, and 5:1 signify [EO]/[Li] ratios). Reproduced from ref 8 with permission. Copyright 2016 American Chemical Society. (e) Chemical structure of comblike PNG−PTG-PNG. TEM images of thin film for (f,g) PNG_7-PTG_{96}-PNG_7 ($f_{wt,PNG}$ = 9.2 wt %) and (h,i) PNG_{18}-PTG_{107}-PNG_{18} ($f_{wt,PNG}$ = 28.6 wt %) doped with LiTFSI. Compared to CP with low PNG fraction, CP with high PNG fraction showed obvious cylindrical domains composed of crystalline PNG chains, demonstrating the formation of Li^+ transport channels; this implied the Li^+ transport channels could be constructed by tuning the ratio of the two kinds of polymers with different hydrophilicity. Reproduced from 33 with permission. Copyright 2018 American Chemical Society.

segmental motion, creating abundant free volumes, through which Li^+ hops from sites to sites accompanied by polymer segmental motion under electric field. The hopping could happen along the polymer chain (intrachain hopping) or between two polymer chains (interchain hopping) with or without the assistance of counterions. According to the mechanism, ionic transport in PEs is influenced by the Li^+ dissociation capability from lithium salt, the coordination capability of polymer polar groups with Li^+, and the polymer chain mobility.

Polymer chain mobility is generally the determining factor of Li^+ conductivity in PEs. Polymer segmental motion is derived from the bond rotation along with polymer conformation transformation, which occurs in the amorphous domains of polymers at temperatures above T_g.[5] Therefore, restrained crystallization, low T_g, and low degrees of chain entanglement of polymers play significant roles in increasing the ionic conductivity of PEs. Polymer crystallization and T_g highly depend on the polymer composition and architecture. For example, Si−O−Si has a large bond angle and long bond length (0.164 nm), thereby exhibiting a low energy barrier of bond rotation and consequent flexibility with a low T_g. However, good flexibility also benefits the folding and crystallization of polymer chains, such as PEO. Creating irregularity in polymers can effectively confine crystal growth, among which constructing branched architecture displays superiority ascribed to the lessened limitation of polymer composition. As mentioned in Section 1, at the same polymer MWs, BPs have shorter linear chains than linear polymers; this translates into remarkably alleviated chain folding and crystallization. More importantly, branching sites, as well as cores or backbones, can act as defects to be relegated to the crystal surfaces, further impeding crystal growth.[6] Additionally, the large number of chain ends in BPs can increase segmental mobility due to their dangling feature and conformational freedom; as a result, BPs can have decreased T_g.[8] Moreover, the shorter chains and unique topologies of BPs (e.g., starlike, bottlebrush-like architecture) also reduce chain entanglement.[7]

In general, the MWs, branching densities, and end groups of BPs affect their chain mobility and the subsequent BP-PE ionic conductivity. Chen and co-workers demonstrated lower T_g and higher ionic conductivity could be achieved by decreasing the MW and raising the branching density of BPs (Figure 4a,b), implying the significant impacts of branched architecture on Li^+ transport.[43] The inhibiting effects of BPs on crystallization have also been exposed; the X-ray diffraction peaks of SP-GPEs, in addition to already being much wider than that of the linear analogue, were found to weaken as the SP arm number rose.[44] Furthermore, bulky end groups were also proven to benefit crystallization suppression and Li^+ transport.[11]

Apart from MWs, branching densities, and end groups, it is worth noting that the influences of core or backbone properties on Li^+ transport need to be considered when their volume/mass fraction in BPs is high. Horike and co-workers used coordination star polymers (CSP) composed of large metal−organic polyhedra cores and PEG arms (Figure 4c) to

https://doi.org/10.1021/acs.nanolett.1c02558
Nano Lett. 2021, 21, 7435−7447

Table 1. Physical Properties, Mechanical Properties, and Electrochemical Performance of SP-PEs

core	arm	[EO]/[Li][a]	T_g[b]	σ[c]	t_{Li^+}[d]	G'[e]	T_d[f]	V[g]	ref
lignin	PPEGMA-*r*-PGMA[h]	14	−18	3.3×10^{-5} (30)		4 (60 °C)		5	13
HBPS	PB[i]-PPEGMA	/	−52	9.63×10^{-5} (30)	0.21		378	5.2	15
trimethylolpropane	PPEGMA-*r*-PGMA[h]	16	−56.2	5.6×10^{-5} (25)	0.37	20 (20 °C)	350	4.5	12
pentaerythritol tribromide	PS/PEO (miktoarm)	16	−43.1	$\sim 10^{-5}$–10^{-6} (25)		~10 (40 °C)			20
HPG[j]	PCL[k]-$(LC)_x$	25 wt % LiTFSI	−43.8	5.98×10^{-5} (30)	0.63 (60 °C)		368	5.12	19
*hb*PPEGMA	PS	16	−46.8	9.5×10^{-5} (60)	0.22 (60 °C)	0.5 (60 °C)		4.34	21
HBPS	PPEGMA	26	−57.5	2.4×10^{-5} (30)			318	5.1	22

[a]The mole ratio of ethylene oxide (EO) unit to Li^+. [b]The glass transition temperature, °C. [c]The ionic conductivity, S cm^{-1} (testing temperature, °C). [d]The Li^+ transference number. [e]The storage modulus, MPa. [f]The onset degradation temperature, °C. [g]The oxidation voltage, V. [h]PGMA: poly(glycidyl methacrylate). [i]PB: poly(pinacol vinylboronate). [j]HPG: hyperbranched poly(glycidol). [k]PCL: poly(ε-caprolactone).

Table 2. Physical Properties, Mechanical Properties, and Electrochemical Performance of CP-PEs

backbone	side chain	[EO]/[Li][a]	T_g[b]	σ[c]	t_{Li^+}[d]	G'[e]	T_d[f]	V[g]	ref
P(PO/EM)[h,i]		16	−29.9	0.7×10^{-5} (30)	0.59		135	4.6	30
PMHS	TMVS/4-BBE[j]	20	N/P	6.6×10^{-4} (30)				3.95	25
PEaMA	Jeffamine	20	−57	1.4×10^{-4} (30)	0.15	$\sim 10^{-4}$ (25 °C)	353	3.8	31
PPEGDA[k]	PEGMA	20	−49.7	5.05×10^{-5} (RT)	0.312		331	5.05	32
PMHS	SBSILi[l]/PEG	28	−60	3.77×10^{-5} (30)	0.80		200	5.2	26
PNG−PTG−PNG[h]		20	−40	9.5×10^{-5} (30)			390		33

[a]The mole ratio of EO unit to Li^+. [b]The glass transition temperature, °C. [c]The ionic conductivity, S cm^{-1} (testing temperature, °C). [d]The Li^+ transference number. [e]The storage modulus, MPa. [f]The onset degradation temperature, °C. [g]The oxidation voltage, V. [h]CPs without indicating backbones and side chains signify CPs synthesized by the "grafting-through" route. [i]P(PO/EM): poly[propylene oxide-*co*-2-(2-methoxyethoxy)-ethyl glycidyl ether]. [j]TMVS/4-BBE: tris(2-methoxyethoxy) vinylsilane/4-bromo-1-butene. [k]PPEGDA: poly(poly(ethylene glycol) diacrylate). [l]SBSILi: lithium 4-styrenesulfonyl (perfluorobutylsulfonyl) imide.

Table 3. Physical Properties, Mechanical Properties, and Electrochemical Performance of BBP-PEs

backbone	brush	[EO]/[Li][a]	T_g[b]	σ[c]	t_{Li^+}[d]	G'[e]	T_d[f]	V[g]	ref
cellulose	PPEGMA		−38	8.00×10^{-5} (30)	0.24		278	4.9	29
P(PEOMA-TFSI$^-$Li$^+$)[h,i]		10.5	−24	1.02×10^{-4} (90)	0.99 (60 °C)	7.4×10^{-5} (90 °C)			39
P*t*BBMA[j]	PPEGMA	16	−48.9	4.49×10^{-5} (30)	0.6 (60 °C)	2.6 (tensile strength)	310	4.8	28
poly(MA)[k]	PEGME[m]	16	−48	9.2×10^{-5} (25)	0.19		350	3.5	38
poly(Nb)[l]	PEGME	16	−48	5.0×10^{-5} (25)	0.13		350	3.5	38
poly(Nb)	PS/PEO	10	−45	$\sim 10^{-3}$ (105)		10^{-2} (45 °C)			40

[a]The mole ratio of EO unit to Li^+. [b]The glass transition temperature, °C. [c]The ionic conductivity, S cm^{-1} (testing temperature, °C). [d]The Li^+ transference number. [e]The storage modulus, MPa. [f]The on-set degradation temperature, °C. [g]The oxidation voltage, V. [h]BBPs without indicating backbones and brushes signify BBPs synthesized by the "grafting-through" route. [i]P(PEOMA-TFSI$^-$Li$^+$): poly(poly(ethylene glycol) methacrylate-TFSI$^-$Li$^+$). [j]P*t*BBMA: poly(*tert*-butyl 2-((2-bromopropionyloxy)methyl) acrylate). [k]poly(MA): polymethacrylate. [l]poly(Nb): polynorbornene. [m]PEGME: poly((ethylene glycol) monomethyl ether).

reveal that the T_g of SPs were dramatically higher than that of the individual arm when the volume fraction of the core was as high as 0.64.[8] In contrast, the T_g values of CSPs with higher arm volume fractions were similar to that of the respective arms and were dominated by the packing structure of the CSPs.[8] Consequently, the ionic conductivity of CSP-based SPEs increased with increasing arm volume fraction (Figure 4d).[8]

3.1.2. Construction of Lithium Ion Transport Channels. Besides designing macromolecular architectures to enhance the ionic conductivity, the construction of Li^+ transport channels inside the bulk PEs is also valuable. These channels not only provide continuous Li^+ transport but also increase local Li^+ concentration because only the interior of the channels contain lithium-conducting chains that solvate Li^+. This manifests itself as reduced practical volumes of PEs in which Li^+ is located. As mentioned in Sections 1 and 2.1, high Li^+ concentration increases ionic conductivity; hence, the channels can further accelerate Li^+ transport. These channels can be constructed through microphase separation originating from BP self-assembly, which is generally induced by the incorporation of two kinds of polymers with different hydrophilicity. For example, Lee and co-workers synthesized a series of poly(2-naphthyl glycidyl ether)-*block*-poly[2-(2-(2-methoxyethoxy)-ethoxy)ethyl glycidyl ether]-*block*-poly(2-naphthyl glycidyl ether) (PNG−PTG−PNG) triblock comblike copolymers with different block compositions (Figure 4e).[33] At the same [Li]/[EO] ratio, the ionic conductivity of SPE increased with PNG fraction and reached the highest value of 9.5×10^{-5} S cm^{-1} at the PNG fraction of 28.6 wt %, which was contributed from the gradually formed Li^+ transport channels (Figure 4f–i). The PNG domains with cylindrical structure were locally oriented in the soft PTG matrices, acting as channel walls to shorten Li^+ pathways, demonstrating the effectiveness of micro phase separation toward ion conduction.

Decorating BPs with functional liquid-crystal units creates a special situation with regards to constructing Li^+ transport channels via microphase separation since liquid crystals can orientate after annealing. By introducing liquid crystals (e.g., poly(4-cyanobiphenyl methyl methacrylate) ($(LC)_x$),[19] poly-

https://doi.org/10.1021/acs.nanolett.1c02558
Nano Lett. 2021, 21, 7435−7447

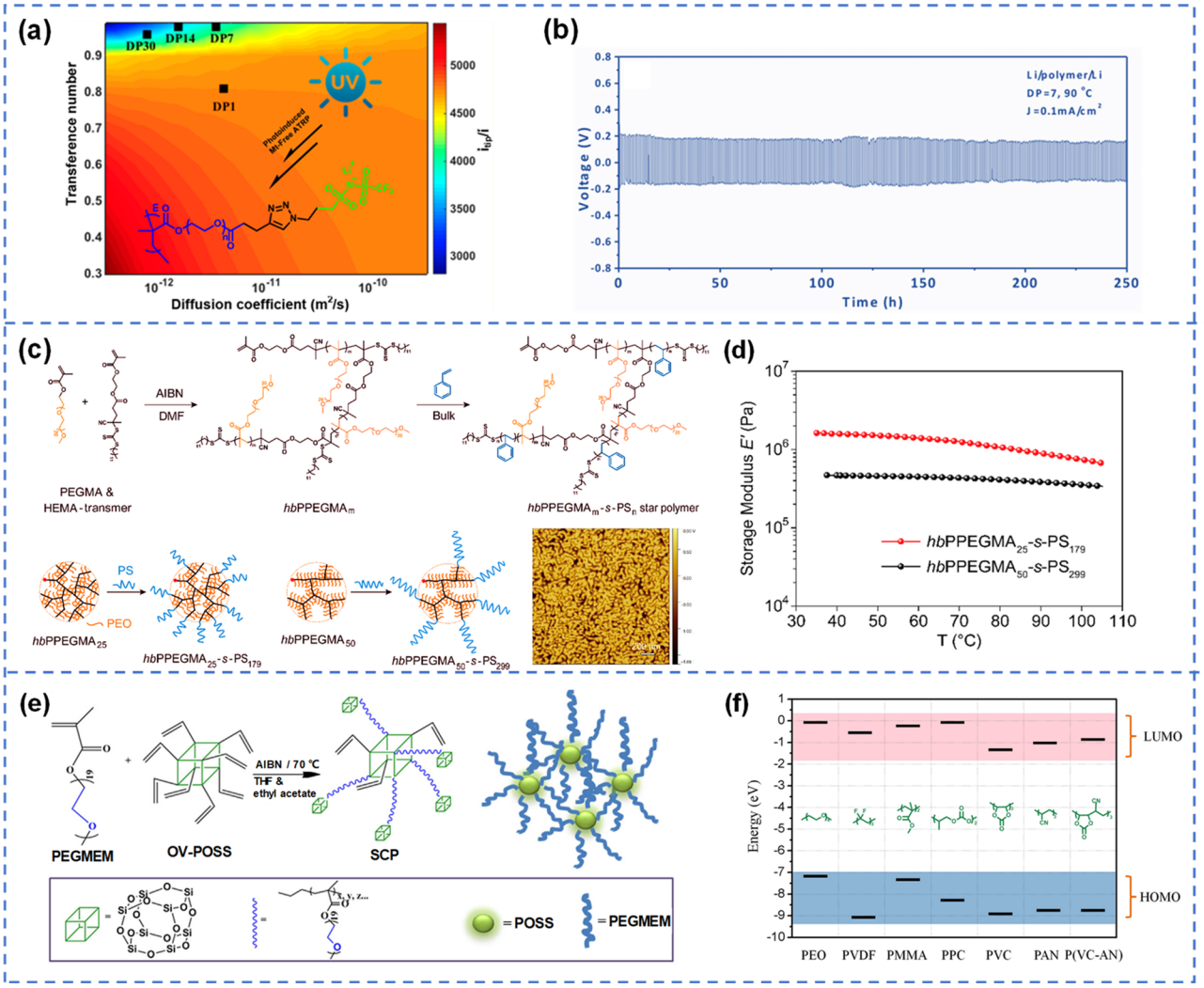

Figure 5. (a) Propensity of dendrite growth (ratio of tip current i_{tip} to applied current (i) for electrolytes under various Li^+ transference numbers and diffusion coefficients at 90 °C. The black squares represent the single-ion conducting CPs synthesized in this work (DP: degrees of polymerization). (b) Lithium stripping−plating performance of DP 7 at the temperature of 90 °C and current density of 0.1 mA cm^{-2}. Reproduced from ref 39 with permission. Copyright 2018 American Chemical Society. (c) Synthetic route and schematic of *hb*PPEGMA$_m$-*s*-PS$_n$ (m and n: average chain length of PEO segments and PS arms, respectively), as well as the AFM image of *hb*PPEGMA$_{50}$-*s*-PS$_{299}$ SPE film. (d) Storage moduli of *hb*PPEGMA$_m$-*s*-PS$_n$ SPEs. Reproduced from ref 21 with permission. Copyright 2019 American Chemical Society. (e) Synthetic route to SPs with POSS as the core and PPEGMA as the arms. Reproduced from ref 49 with permission. Copyright 2016 Elsevier B.V. (f) Frontier orbital energy levels of polymer matrixes in reported SPEs matched with LNMO cathodes. Reproduced from ref 50 with permission. Copyright 2019 American Chemical Society.

{2,5-bis[(4-methoxyphenyl) oxycarbonyl] styrene} (PMPCS)[37]) into lithium-conducting BPs, the orientation ability of liquid crystals can drive the branched copolymer to have (local) ordered arrangement, boosting the assembly of lithium-conducting polymers into continuous channels. Notably, the position of liquid crystals in the BPs may influence the channel formation. For example, liquid crystal chains anchored on the outer shell of SPs were demonstrated to generate ordered domains with a lamellar structure.[45] Nevertheless, liquid crystal chains on the inner sphere struggled to interact with each other, rendering discontinuous packing in the polymer.

3.2. Ion Transference Number. As mentioned in Section 1, ionic conductivity is the sum of the behaviors of all ion species within the electrolytes. However, only Li^+ can be involved in the electrochemical reactions with electrodes for energy storage in lithium-based batteries. Therefore, the fraction of ionic current carried by Li^+, which reflects the charge transport efficiency, is crucial and can be evaluated by Li^+ transference number. BPs generally possess promoted Li^+ transference numbers owing to their accelerated Li^+ transport (Tables 1−3); however, constructing single-ion conducting BPs by copolymerization is still the most effective way to reach high Li^+ transference numbers. Single-ion conducting polymers usually have anionic moieties anchored on the chains that could be coordinated with Li^+, acting as lithium reservoirs, or have anion acceptors on the chains which could partially immobilize anions. Common anionic moieties are usually derived from the anions of conventional lithium salt, such as $-SO_2N^{(-)}SO_2CF_3$, $-SO_2N^{(-)}SO_2F$, $-SO_3^-$, $-OB^{(-)}(O)(C_2O_4)$, and $-CO_2^-$, while anion acceptors are mainly boron and calix[6]pyrrole-based Lewis acids.[46] For example, a comblike block copolymer composed of poly(lithium 1-[3-(methacryloyloxy)-propylsulfonyl]-1-(trifluoromethylsulfonyl)-

https://doi.org/10.1021/acs.nanolett.1c02558
Nano Lett. 2021, 21, 7435−7447

imide) (LiMTFSI) and PEGMA was reported to have an increased Li^+ transference number of 0.83 at RT and a comparable ionic conductivity of 1.2×10^{-5} S cm^{-1} at 55 °C.[47] It is worth noting that, a promoted Li^+ transference number is also crucial for lithium dendrite suppression. Matyjaszewski and co-workers proposed that for a defect-free system at constant ion diffusion coefficients the increased Li^+ transference number could lead to an enhancement of lithium dendrite suppression by 3−4 times (Figure 5a).[39] As a result, the synthesized single-ion conducting CP with Li^+ transference number as high as 0.99 at 90 °C provided stable lithium stripping−plating (Figure 5b) and suppressed lithium dendrite.

3.3. Mechanical Property. Although BPs have advantages over linear polymers regarding ionic conductivity, they normally possess poor mechanical strength and moduli ascribed to the low degree of chain entanglement. Therefore, the trade-off between mechanical properties and ionic conductivity is vital. Up until now, there are four ways to enhance the mechanical robustness of BP-PEs: crafting block copolymers, constructing inorganic/organic hybrid materials, using rigid network as matrices, and cross-linking.

Branched block copolymers for PEs fundamentally consist of two parts: (1) polymers with high T_g to provide mechanical robustness and (2) soft polymers to serve as lithium conductors. The disparate hydrophilicity of the two kinds of polymers can induce microphase separation, as mentioned in Section 3.1.2. Polymers containing aromatic rings, especially PS, are commonly used for mechanical enhancement because the steric hindrance of the aromatic rings impede bond rotation. Many BAB-type CPs and BBPs have been reported, including PS-*b*-PPEGMA-*b*-PS,[48] PNG−PTG-PNG,[33] poly-[(norbornene-*graft*-styrene)-*block*-(norbornene-*graft*-ethylene oxide)-*block*-(norbornene-*graft*- styrene)] (*g*PS-*g*PEO-*g*PS),[40] and so forth which not only maintained PE ionic conductivities of 10^{-3}−10^{-5} S cm^{-1} but also exhibited desirable mechanical properties with elastic moduli reaching ∼10^{-2}−1 MPa. A hyperbranched SP with PPEGMA cores and PS arms was also constructed (*hb*PPEGMA-*s*-PS) (Figure 5c).[21] The corresponding SPE exhibited a decent storage modulus of 0.5 MPa (Figure 5d) and ionic conductivity of 9.5×10^{-5} S cm^{-1} at 60 °C. The second effective approach to promote the mechanical properties of BP-PEs is the incorporation of inorganic components. Besides direct physical blending, introducing structured inorganic materials into the polymer framework, especially as the cores or backbones of the BPs, is reliable. POSS is a typical inorganic/organic hybrid material, consisting of silicon/oxygen framework in the center and organic groups at each corner connected with silicon, which could be easily functionalized (Figure 5e).[49] Nevertheless, it is worth noting that the rigid inorganic cores/backbones can enhance the mechanical properties only when their volume/mass fractions in BPs are high.

Physically confining BPs into a relatively rigid network, such as poly(vinylidene fluoride-hexafluoropropylene) (PVDF-HFP) and PVDF, is another way to balance the ionic conductivities and mechanical properties. On the one hand, chains in BPs with unchanged flexibility still have sufficient space to move for ion conduction. On the other hand, the robust network can provide adequate strength to maintain PE integrity. Confining polymers in nanoscale spaces is a structural strategy with rising popularity in recent years, as polymers show decreased crystallinity and promoted chain segmental dynamics.[11,22] Finally, the mechanical properties of BPs can be enhanced by cross-linking.[13] Cross-linking could restrain the segmental motion of polymers; therefore, it is preferable to cross-link polymers through independent and dangling cross-linking functional groups on the main chains with optimized cross-linking densities while maintaining the flexibility and conformational freedom of the lithium-conducting side chains.

3.4. Thermal Stability. Good thermal stabilities (>180 °C) of PEs are of key importance for practical batteries considering the safety issues and the rising demands of high-operation-temperature batteries. Polymers with higher MWs normally have better thermal stabilities.[32] Accordingly, branching may lead to the decrease of polymer degradation temperature, especially when the chemical bonds in branching sites are weak. However, this disadvantage can be compensated by chemical composition engineering and structure regulation (Tables 1−3). Specifically, the spatial configuration of polymers can influence the polymer degradation. For example, isotactic polylactides (PLAs) are thermally more stable than the atactic analogues at the same MW.[17] Furthermore, introducing thermally stable components (e.g., aromatic rings, inorganic compounds) and cross-linking BPs both increase the degradation temperature of BP-PEs. Additionally, removing thermally unstable moieties (e.g., −COOH) and/or anchoring functional groups with high bonding energy (e.g., $-CF_3$) also impart beneficial effects toward improving thermal stabilities.[14] It is worth noting that when the mass/volume fraction of core/backbone is high, constructing BPs can actually increase the thermal stability as a result of the stable cores or backbones. Above all, there are two points which should be paid attention: (1) enhanced thermal stabilities normally signify increased T_g and crystallinity, so the balance of polymer ionic conductivities and thermal stabilities is essential; (2) although polymers with high degradation temperature induced by rigid chains also have high mechanical strength, thermal stabilities and mechanical properties are not necessarily related.

3.5. Interfacial Chemistry and Electrochemical Stability. Compared to solid ceramic electrolytes, PEs possess numerous merits, including better flexibility to maintain intimate interfacial contacts and relatively more stable electrode−electrolyte interfaces.[51] However, large interfacial impedance that originated from interfacial instability can still be observed in PEs. The instability resulted from two types of reactions: (1) spontaneous interfacial reaction when PEs are in contact with electrodes, and (2) electrochemical decomposition of PEs during cycling. Generally, PEs with lower highest occupied molecular orbital (HOMO) and higher lowest unoccupied molecular orbital (LUMO) energy levels exhibit higher stabilities against cathodes and anodes, respectively (Figure 5f).[50] For the cathode side, if the Fermi energy of the cathode is below the HOMO of PEs, PEs will be locally oxidized.[52] Similarly, for the anode side if the Fermi energy of the anode is above the LUMO of PEs, PEs will be locally reduced.[52] For example, PPC could be degraded when in contact with Li metal, forming solid-electrolyte interphase (SEI) layer.[53] However, in some cases if the SEI layer is thin and controllable the interfacial resistance will be reduced due to the enhanced contact between the electrode and PE. In recent years, the energy level of ionic species is also considered to study the interfacial reaction. At the electrode−electrolyte interfaces, the Li^+ could diffuse across solid−electrolyte interface from the position with higher Li^+ chemical potential to that with lower Li^+ chemical potential, resulting in the

https://doi.org/10.1021/acs.nanolett.1c02558
Nano Lett. 2021, 21, 7435−7447

formation of space charge layer. This Li^+ migration is commonly seen at cathode−electrolyte interfaces.

Additionally, during cycling the cathode−PE and anode−PE interfaces have highly oxidized and reduced environment, respectively, which could further accelerate the interfacial side reactions and decomposition of PEs. Therefore, the compatibility of PEs with electrode, particularly with cathode is essential. However, conventional PEs, especially ether-based PEs have inferior antioxidized ability, which reduces the cycling life of high-voltage cathode-based battery (e.g., 4.45 V-class $LiCoO_2$ and 4.7 V-class spinel $LiNi_{0.5}Mn_{1.5}O_4$) and limits the battery energy density.[54] BP-PEs generally show an enlarged voltage window with oxidation voltage higher than 4−4.2 V, whereas linear PEO oxidizes at ∼3.9 V, demonstrating that structural regulation has positive impacts on improving the electrochemical stability of PEs. However, to further increase the antioxidation ability of BPs, the design of polymer components is crucial. Compared with branched polyether PEs, BP-PEs containing polycarbonates and polyesters have better antioxidation abilities. Furthermore, modifying BPs with high-polarity groups tends to decrease the lower HOMO energy level and increase the oxidation voltage,[50] such as introducing −CN as the end groups of SP arms.[19] Additionally, the antioxidation ability of branched PEs can be enhanced by introducing components that absorb impurities, such as B atoms, which have empty p-orbitals,[15] and carbon materials.

4. SUMMARY AND OUTLOOK

This Mini Review presents an overview of lithium-conducting BPs for PEs by critically examining the type and effect of BP chain architectures, and effective strategies for enhancing their ionic conductivity, ion transference number, mechanical properties, thermal stability, and interfacial chemistry and electrochemical stability. The unique architectures of SPs, CPs, BBPs and HBPs are discussed. In contrast to linear analogues, branched topologies can effectively decrease T_g, crystallinity, and chain entanglement of polymers, imparting them with higher segmental mobility and larger amorphous area. Generally, a relatively high branching density and short branched-chain length in BPs facilitate lithium transport of PEs with ionic conductivity of 10^{-3}−10^{-5} S cm^{-1}. More importantly, when the mass (or volume) fractions of the core/backbone of BPs are high, their properties (e.g., rigidity and thermal stability) greatly impact the chain dynamics and the physical and mechanical properties of BP-PEs. BPs also manifest relatively increased Li^+ transference number and electrochemical stability, yet the promoted Li^+ transport ability sacrifices mechanical modulus and thermal stability; however, this can be compensated via the introduction of high-T_g and thermally stable components in PEs or by simply cross-linking BPs. Nevertheless, there is still much to be addressed and exciting opportunities to be identified prior to the utilization and commercialization of BP-PEs in batteries.

(1) BPs employed for PEs often lack both thorough characterization and precisely controlled architectures (e.g., grafting density, branching chain length and uniformity, core/backbone sizes, PDI), due partially to the complicated synthetic process, tedious postprocessing, and low yield. Clearly, the architecture effects of BPs on electrochemical performance need to be further scrutinized. Moreover, in-depth experimental analysis of the electrochemical behaviors of BP-PEs (e.g., oxidation reactions of BP-PEs at high voltages and associated influencing factors, interfacial electrochemical reactions of BP-PEs with cathodes and anodes) in conjunction with theoretical modeling and simulation is required. Notably, a surprisingly limited number of studies involve systematic comparison of the impacts of different topologies of BP-PEs on electrochemical performance, which is due largely to their complex synthesis; this opens several new opportunities for future exploration.

(2) Constructing branched architectures could effectively increase the ionic conductivities of polymers by even 1−2 orders of magnitude over linear counterparts, yet their RT conductivities still fall below the targeted value issued by USABC (i.e., 1×10^{-3} S cm^{-1} for PEs conducting two or more ions, and 1×10^{-4} S cm^{-1} for PEs conducting single ion). The ability to judiciously regulate and optimize BP architectures, as noted in (1), renders the possibility to further promote their ionic conductivity. Peculiarly, some of the unique features of BBP-PEs (e.g., high grafting density, readily self-assembling into ordered structures via structural and compositional tailoring) may have unexpected impacts on the ionic conductivity of PEs. Although their reported performance is lower than expected, BBPs are still recognized to hold great potential due to the brush-composed Li^+ transport channels. In addition to tuning the brush MWs, the backbone length of BBPs also has significant impact and should be delicately controlled. Moreover, it is worth noting that because of strong steric hindrance between adjacent brushes the initiation efficiency and actual grafting density of BBPs need to be evaluated, especially when using macromonomers (e.g., PEGMA) or presynthesized polymer chains as grafting units. Additionally, creating branched architectures containing other lithium-conducting polymers (e.g., polycarbonate and PIL) instead of ether-based polymers and modulating polymer composition also provides opportunities to increase the ionic conductivity of PEs. Apart from transporting Li^+, BPs conducting other metal ions (e.g., Na^+, K^+, Zn^{2+}) could be developed as well to expand the applications of BP-PEs to other solid-state metal-ion batteries.

(3) Crafting branched polymers/inorganics for composite PEs represents another promising strategy to enhance the performance of SSEs. Either inert fillers or fast-ion-conductive inorganics can facilitate lithium transport. Several structures such as polymer-in-ceramic, polymer−inorganic−polymer-sandwiched structures, and vertically aligned inorganic nano-channels,[9] which have been successfully demonstrated by employing linear polymers, can be constructed by utilizing BPs. Notably, the compatibility of inorganic and polymer components is of key importance in ensuring continuous Li^+ transport pathways. Grafting oligomers or polymers on the surface of inorganic particles has been demonstrated to effectively promote the compatibility and ionic conductivity of composite PEs.[55] In this regard, amphiphilic branched diblock copolymers, such as starlike block copolymers and bottlebrush-like block copolymers synthesized via sequential ATRP of respective monomers, are uniquely positioned as they can readily function as nanoreactors for the *in situ* growth of inorganic nanoparticles and nanorods, respectively. Thus, they are capable of yielding an assortment of nanocrystals with polymers intimately and permanently tethered on the surface.[56,57] This contrasts sharply to the case where polymers are ligand-exchanged onto the surface of nanocrystals, in which the possible dissociation of capped polymers and thus aggregation of nanocrystals over time can occur. Moreover, by rationally

https://doi.org/10.1021/acs.nanolett.1c02558
Nano Lett. 2021, 21, 7435−7447

tuning the compositions and architectures of branched block copolymer nanoreactors, core/shell and hollow nanocrystals can be conveniently crafted.[56,57] More importantly, such polymer-ligated nanocrystals, which offer controllable grafting density of polymer chains on the surface due to the use of well-defined core or backbone molecules for the nanoreactor synthesis,[56,57] render possible systematic investigation into the effect of the number of arms/brushes on the physical and mechanical properties of composite PEs. Furthermore, in addition to being individually used as PEs, BPs can also perform as buffer layers sandwiched between inorganic SSE and electrodes to increase the wettability and contact.

(4) Prior studies have focused primarily on the molecular architecture and composition design of BPs, whereas the scrutiny of the morphology of resulting BP-PE films or gels is largely overlooked. It is notable that capitalizing on the self-assembly of BPs may afford an effective platform to construct lithium transport channels. Various self-assembled morphologies and structures can be yielded by precisely tuning the shape of amphiphilic BPs. Additionally, creating vertically oriented lithium transport channels in PE films or gels between two electrodes may also be feasible and significant via self-assembly of BPs under the application of external electric field.

In summary, BPs present great potential for use in PEs owing to their low viscosity and high chain segmental motion. Their tunable and controllable architecture confers BPs a set of intriguing properties and, thus, significant room for performance improvement. Further efforts are still needed regarding the design, synthesis, and characterization of BPs ranging from macromolecular structure to assemblies. With the necessary development of synthesis and evaluation techniques, as well as in-depth understanding of BP-related electrochemical mechanisms with insights provided by computation and simulation, the crafting and implementation of BPs as PEs will remain an active area of exploration for next-generation lithium batteries and, by extension, other metal batteries.

AUTHOR INFORMATION

Corresponding Authors

Caizhen Zhu − *Institute of Low-Dimensional Materials Genome Initiative, College of Chemistry and Environmental Engineering, Shenzhen University, Shenzhen, Guangdong 518060, P.R. China;* orcid.org/0000-0002-7330-8300; Email: czzhu@szu.edu.cn

Zhiqun Lin − *School of Materials Science and Engineering, Georgia Institute of Technology, Atlanta, Georgia 30332, United States;* orcid.org/0000-0003-3158-9340; Email: zhiqun.lin@mse.gatech.edu

Authors

Shu-Meng Hao − *Institute of Low-Dimensional Materials Genome Initiative, College of Chemistry and Environmental Engineering, Shenzhen University, Shenzhen, Guangdong 518060, P.R. China; School of Materials Science and Engineering, Georgia Institute of Technology, Atlanta, Georgia 30332, United States*

Shuang Liang − *School of Materials Science and Engineering, Georgia Institute of Technology, Atlanta, Georgia 30332, United States*

Christopher D. Sewell − *School of Materials Science and Engineering, Georgia Institute of Technology, Atlanta, Georgia 30332, United States*

Zili Li − *School of Materials Science and Engineering, Georgia Institute of Technology, Atlanta, Georgia 30332, United States*

Jian Xu − *Institute of Low-Dimensional Materials Genome Initiative, College of Chemistry and Environmental Engineering, Shenzhen University, Shenzhen, Guangdong 518060, P.R. China;* orcid.org/0000-0002-9370-4829

Complete contact information is available at: https://pubs.acs.org/10.1021/acs.nanolett.1c02558

Notes

The authors declare no competing financial interest.

ACKNOWLEDGMENTS

This work is supported by the NSF (Chemistry 1903957) and AFOSR (FA9550-19-1-0317).

REFERENCES

(1) Liu, M.; Zhou, D.; He, Y. B.; Fu, Y. Z.; Qin, X. Y.; Miao, C.; Du, H. D.; Li, B. H.; Yang, Q. H.; Lin, Z. Q.; Zhao, T. S.; Kang, F. Y. Novel gel polymer electrolyte for high-performance lithium-sulfur batteries. *Nano Energy* **2016**, *22*, 278−289.

(2) Lu, Q. W.; He, Y. B.; Yu, Q. P.; Li, B. H.; Kaneti, Y. V.; Yao, Y. W.; Kang, F. Y.; Yang, Q. H. Dendrite-Free, High-Rate, Long-Life Lithium Metal Batteries with a 3D Cross-Linked Network Polymer Electrolyte. *Adv. Mater.* **2017**, *29*, 1604460.

(3) Lei, D. N.; He, Y. B.; Huang, H. J.; Yuan, Y. F.; Zhong, G. M.; Zhao, Q.; Hao, X. G.; Zhang, D. F.; Lai, C.; Zhang, S. W.; Ma, J. B.; Wei, Y. P.; Yu, Q. P.; Lv, W.; Yu, Y.; Li, B. H.; Yang, Q. H.; Yang, Y.; Lu, J.; Kang, F. Y. Cross-linked beta alumina nanowires with compact gel polymer electrolyte coating for ultra-stable sodium metal battery. *Nat. Commun.* **2019**, *10*, 4244.

(4) Fan, F.; Wang, W. Y.; Holt, A. P.; Feng, H. B.; Uhrig, D.; Lu, X. Y.; Hong, T.; Wang, Y. Y.; Kang, N. G.; Mays, J.; Sokolov, A. P. Effect of Molecular Weight on the Ion Transport Mechanism in Polymerized Ionic Liquids. *Macromolecules* **2016**, *49*, 4557−4570.

(5) Zhao, Q.; Stalin, S.; Zhao, C. Z.; Archer, L. A. Designing Solid-State Electrolytes for Safe, Energy-Dense Batteries. *Nat. Rev. Mater.* **2020**, *5*, 229−252.

(6) Stowe, M. K.; Liu, P.; Baker, G. L. Star Poly(ethylene oxide) as a Low Temperature Electrolyte and Crystallization Inhibitor. *Chem. Mater.* **2005**, *17*, 6555−6559.

(7) Hosono, N.; Gochomori, M.; Matsuda, R.; Sato, H.; Kitagawa, S. Metal-Organic Polyhedral Core as a Versatile Scaffold for Divergent and Convergent Star Polymer Synthesis. *J. Am. Chem. Soc.* **2016**, *138*, 6525−6531.

(8) Nagarkar, S. S.; Tsujimoto, M.; Kitagawa, S.; Hosono, N.; Horike, S. Modular Self-Assembly and Dynamics in Coordination Star Polymer Glasses: New Media for Ion Transport. *Chem. Mater.* **2018**, *30*, 8555−8561.

(9) Tang, S.; Guo, W.; Fu, Y. Z. Advances in Composite Polymer Electrolytes for Lithium Batteries and Beyond. *Adv. Energy Mater.* **2021**, *11*, 2000802.

(10) Lopez, J.; Mackanic, D. G.; Cui, Y.; Bao, Z. N. Designing Polymers for Advanced Battery Chemistries. *Nat. Rev. Mater.* **2019**, *4*, 312−330.

(11) Yao, Y.; Sakai, T.; Steinhart, M.; Butt, H. J.; Floudas, G. Effect of Poly(ethylene oxide) Architecture on the Bulk and Confined Crystallization within Nanoporous Alumina. *Macromolecules* **2016**, *49*, 5945−5954.

(12) Tong, Y. F.; Lyu, H. L.; Xu, Y. Z.; Thapaliya, B. P.; Li, P. P.; Sun, X. G.; Dai, S. All-Solid-State Interpenetrating Network Polymer Electrolytes for Long Cycle Life of Lithium Metal Batteries. *J. Mater. Chem. A* **2018**, *6*, 14847−14855.

(13) Jeong, D.; Shim, J.; Shin, H.; Lee, J. C. Sustainable Lignin-Derived Cross-Linked Graft Polymers as Electrolyte and Binder

Materials for Lithium Metal Batteries. *ChemSusChem* **2020**, *13*, 2642−2649.
(14) Xu, H.; Wang, A.; Liu, X.; Feng, D.; Wang, S.; Chen, J.; An, Y.; Zhang, L. A New Fluorine-Containing Star-Branched Polymer as Electrolyte for All-Solid-State Lithium-Ion Batteries. *Polymer* **2018**, *146*, 249−255.
(15) Wang, S.; Li, J. Y.; Li, Q. Y.; Chen, J.; Liu, X.; Wang, Z. N.; Zeng, Q. H.; Zhao, T.; Liu, X. F.; Zhang, L. Y. Topological Polymer Electrolyte Containing Poly(pinacol vinylboronate) Segments Composited with Ceramic Nanowires towards Ambient-Temperature Superior Performance All-Solid-State Lithium Batteries. *J. Power Sources* **2019**, *413*, 318−326.
(16) Xiao, Z. L.; Zhou, B. H.; Wang, J. R.; Zuo, C.; He, D.; Xie, X. L.; Xue, Z. G. PEO-Based Electrolytes Blended with Star Polymers with Precisely Imprinted Polymeric Pseudo-Crown Ether Cavities for Alkali Metal Ion Batteries. *J. Membr. Sci.* **2019**, *576*, 182−189.
(17) Ren, J. M.; McKenzie, T. G.; Fu, Q.; Wong, E. H.; Xu, J.; An, Z.; Shanmugam, S.; Davis, T. P.; Boyer, C.; Qiao, G. G. Star Polymers. *Chem. Rev.* **2016**, *116*, 6743−6836.
(18) Goh, T. K.; Coventry, K. D.; Blencowe, A.; Qiao, G. G. Rheology of Core Cross-Linked Star Polymers. *Polymer* **2008**, *49*, 5095−5104.
(19) Wang, S.; Wang, A.; Liu, X.; Xu, H.; Chen, J.; Zhang, L. Ordered Mesogenic Units-Containing Hyperbranched Star Liquid Crystal All-Solid-State Polymer Electrolyte for High-Safety Lithium-Ion Batteries. *Electrochim. Acta* **2018**, *259*, 213−224.
(20) Lee, D.; Jung, H. Y.; Park, M. J. Solid-State Polymer Electrolytes Based on AB_3-Type Miktoarm Star Copolymers. *ACS Macro Lett.* **2018**, *7*, 1046−1050.
(21) Chen, Y.; Shi, Y.; Liang, Y. L.; Dong, H.; Hao, F.; Wang, A.; Zhu, Y. X.; Cui, X. L.; Yao, Y. Hyperbranched PEO-Based Hyperstar Solid Polymer Electrolytes with Simultaneous Improvement of Ion Transport and Mechanical Strength. *ACS Appl. Energy Mater.* **2019**, *2*, 1608−1615.
(22) Chen, P.; Liu, X.; Wang, S.; Zeng, Q.; Wang, Z.; Li, Z.; Zhang, L. Confining Hyperbranched Star Poly(ethylene oxide)-Based Polymer into a 3D Interpenetrating Network for a High-Performance All-Solid-State Polymer Electrolyte. *ACS Appl. Mater. Interfaces* **2019**, *11*, 43146−43155.
(23) Shi, H. F.; Zhao, Y.; Dong, X.; Zhou, Y.; Wang, D. J. Frustrated Crystallisation and Hierarchical Self-Assembly Behaviour of Comb-Like Polymers. *Chem. Soc. Rev.* **2013**, *42*, 2075−2099.
(24) Shi, H. F.; Zhao, Y.; Jiang, S. C.; Rottstegge, J.; Xin, J. H.; Wang, D. J.; Xu, D. F. Effect of Main-Chain Rigidity on the Phase Transitional Behavior of Comblike Polymers. *Macromolecules* **2007**, *40*, 3198−3203.
(25) Hong, J.-H.; Kim, J. W.; Kumar, S.; Kim, B.; Jang, J.; Kim, H.-J.; Lee, J.; Lee, J.-S. Solid Polymer Electrolytes from Double-Comb Poly(methylhydrosiloxane) Based on Quaternary Ammonium Moiety-Containing Crosslinking System for Li/S Battery. *J. Power Sources* **2020**, *450*, 227690.
(26) Ren, C. S.; Liu, M. Z.; Zhang, J. W.; Zhang, Q. H.; Zhan, X. L.; Chen, F. Q. Solid-State Single-Ion Conducting Comb-Like Siloxane Copolymer Electrolyte with Improved Conductivity and Electrochemical Window for Lithium Batteries. *J. Appl. Polym. Sci.* **2018**, *135*, 45848.
(27) Meyer, W. H. Polymer Electrolytes for Lithium-Ion Batteries. *Adv. Mater.* **1998**, *10*, 439−448.
(28) Li, S. Q.; Jiang, K.; Wang, J. R.; Zuo, C.; Jo, Y. H.; He, D.; Xie, X. L.; Xue, Z. G. Molecular Brush with Dense PEG Side Chains: Design of a Well-Defined Polymer Electrolyte for Lithium-Ion Batteries. *Macromolecules* **2019**, *52*, 7234−7243.
(29) Wang, S.; Zhang, L.; Zeng, Q.; Liu, X.; Lai, W.-Y.; Zhang, L. Cellulose Microcrystals with Brush-Like Architectures as Flexible All-Solid-State Polymer Electrolyte for Lithium-Ion Battery. *ACS Sustainable Chem. Eng.* **2020**, *8*, 3200−3207.
(30) Wang, Q. L.; Cui, Z. L.; Zhou, Q.; Shangguan, X. H.; Du, X. F.; Dong, S. M.; Qiao, L. X.; Huang, S. Q.; Liu, X. C.; Tang, K.; Zhou, X. H.; Cui, G. L. A Supramolecular Interaction Strategy Enabling High-Performance All Solid State Electrolyte of Lithium Metal Batteries. *Energy Storage Mater.* **2020**, *25*, 756−763.
(31) Aldalur, I.; Martinez-Ibanez, M.; Krzton-Maziopa, A.; Piszcz, M.; Armand, M.; Zhang, H. Flowable Polymer Electrolytes for Lithium Metal Batteries. *J. Power Sources* **2019**, *423*, 218−226.
(32) Wei, Z.; Chen, S.; Wang, J.; Wang, Z.; Zhang, Z.; Yao, X.; Deng, Y.; Xu, X. Superior Lithium Ion Conduction of Polymer Electrolyte with Comb-Like Structure via Solvent-Free Copolymerization for Bipolar All-Solid-State Lithium Battery. *J. Mater. Chem. A* **2018**, *6*, 13438−13447.
(33) Kim, B.; Chae, C. G.; Satoh, Y.; Isono, T.; Ahn, M. K.; Min, C. M.; Hong, J. H.; Ramirez, C. F.; Satoh, T.; Lee, J. S. Synthesis of Hard-Soft-Hard Triblock Copolymers, Poly(2-naphthyl glycidyl ether)-block-poly[2-(2-(2-methoxyethoxy)ethoxy)ethyl glycidyl ether]-block-poly(2-naphthyl glycidyl ether), for Solid Electrolytes. *Macromolecules* **2018**, *51*, 2293−2301.
(34) Abbasi, M.; Faust, L.; Wilhelm, M. Comb and Bottlebrush Polymers with Superior Rheological and Mechanical Properties. *Adv. Mater.* **2019**, *31*, No. 1806484.
(35) Pelras, T.; Mahon, C. S.; Mullner, M. Synthesis and Applications of Compartmentalised Molecular Polymer Brushes. *Angew. Chem., Int. Ed.* **2018**, *57*, 6982−6994.
(36) Neugebauer, D.; Zhang, Y.; Pakula, T.; Sheiko, S. S.; Matyjaszewski, K. Densely-Grafted and Double-Grafted PEO Brushes via ATRP. A Route to Soft Elastomers. *Macromolecules* **2003**, *36*, 6746−6755.
(37) Ping, J.; Pan, H.; Hou, P. P.; Zhang, M.-Y.; Wang, X.; Wang, C.; Chen, J.; Wu, D.; Shen, Z.; Fan, X.-H. Solid Polymer Electrolytes with Excellent High-Temperature Properties Based on Brush Block Copolymers Having Rigid Side Chains. *ACS Appl. Mater. Interfaces* **2017**, *9*, 6130−6137.
(38) Rosenbach, D.; Modl, N.; Hahn, M.; Petry, J.; Danzer, M. A.; Thelakkat, M. Synthesis and Comparative Studies of Solvent-Free Brush Polymer Electrolytes for Lithium Batteries. *ACS Appl. Energy Mater.* **2019**, *2*, 3373−3388.
(39) Li, S. P.; Mohamed, A. I.; Pande, V.; Wang, H.; Cuthbert, J.; Pan, X. C.; He, H. K.; Wang, Z. Y.; Viswanathan, V.; Whitacre, J. F.; Matyjaszewski, K. Single-Ion Homopolymer Electrolytes with High Transference Number Prepared by Click Chemistry and Photoinduced Metal-Free Atom-Transfer Radical Polymerization. *ACS Energy Lett.* **2018**, *3*, 20−27.
(40) Bates, C. M.; Chang, A. B.; Momcilovic, N.; Jones, S. C.; Grubbs, R. H. ABA Triblock Brush Polymers: Synthesis, Self-Assembly, Conductivity, and Rheological Properties. *Macromolecules* **2015**, *48*, 4967−4973.
(41) Jiang, W. F.; Zhou, Y. F.; Yan, D. Y. Hyperbranched Polymer Vesicles: from Self-Assembly, Characterization, Mechanisms, and Properties to Applications. *Chem. Soc. Rev.* **2015**, *44*, 3874−3889.
(42) Lee, S. I.; Schomer, M.; Peng, H. G.; Page, K. A.; Wilms, D.; Frey, H.; Soles, C. L.; Yoon, D. Y. Correlations between Ion Conductivity and Polymer Dynamics in Hyperbranched Poly(ethylene oxide) Electrolytes for Lithium-Ion Batteries. *Chem. Mater.* **2011**, *23*, 2685−2688.
(43) Zhao, Y.; Ma, M.; Lin, X.; Chen, M. Photoorganocatalyzed Divergent Reversible-Deactivation Radical Polymerization towards Linear and Branched Fluoropolymers. *Angew. Chem., Int. Ed.* **2020**, *59*, 21470−21474.
(44) Zhou, N.; Wang, Y.; Zhou, Y.; Shen, J.; Zhou, Y.; Yang, Y. Star-Shaped Multi-Arm Polymeric Ionic Liquid Based on Tetraalkylammonium Cation as High Performance Gel Electrolyte for Lithium Metal Batteries. *Electrochim. Acta* **2019**, *301*, 284−293.
(45) Tong, Y. F.; Chen, L.; He, X. H.; Chen, Y. W. Sequential Effect and Enhanced Conductivity of Star-Shaped Diblock Liquid-Crystalline Copolymers for Solid Electrolytes. *J. Power Sources* **2014**, *247*, 786−793.
(46) Zhang, H.; Li, C.; Piszcz, M.; Coya, E.; Rojo, T.; Rodriguez-Martinez, L. M.; Armand, M.; Zhou, Z. Single Lithium-Ion Conducting Solid Polymer Electrolytes: Advances and Perspectives. *Chem. Soc. Rev.* **2017**, *46*, 797−815.

https://doi.org/10.1021/acs.nanolett.1c02558
Nano Lett. 2021, 21, 7435−7447

(47) Porcarelli, L.; Shaplov, A. S.; Salsamendi, M.; Nair, J. R.; Vygodskii, Y. S.; Mecerreyes, D.; Gerbaldi, C. Single-Ion Block Copoly(ionic liquid)s as Electrolytes for All-Solid State Lithium Batteries. *ACS Appl. Mater. Interfaces* **2016**, *8*, 10350−10359.
(48) Guan, T. Y.; Qian, S. J.; Guo, Y. K.; Cheng, F. Y.; Zhang, W. Q.; Chen, J. Star Brush Block Copolymer Electrolytes with High Ambient-Temperature Ionic Conductivity for Quasi-Solid-State Lithium Batteries. *ACS Mater. Lett.* **2019**, *1*, 606−612.
(49) Zhang, J.; Ma, C.; Liu, J.; Chen, L.; Pan, A.; Wei, W. Solid Polymer Electrolyte Membranes Based on Organic/Inorganic Nanocomposites with Star-Shaped Structure for High Performance Lithium Ion Battery. *J. Membr. Sci.* **2016**, *509*, 138−148.
(50) Xu, H. T.; Zhang, H. R.; Ma, J.; Xu, G. J.; Dong, T. T.; Chen, J. C.; Cui, G. L. Overcoming the Challenges of 5 V Spinel $LiNi_{0.5}Mn_{1.5}O_4$ Cathodes with Solid Polymer Electrolytes. *ACS Energy Lett.* **2019**, *4*, 2871−2886.
(51) Fan, L.; Wei, S.; Li, S.; Li, Q.; Lu, Y. Recent Progress of the Solid-State Electrolytes for High-Energy Metal-Based Batteries. *Adv. Energy Mater.* **2018**, *8*, 1702657.
(52) Goodenough, J. B. Evolution of Strategies for Modern Rechargeable Batteries. *Acc. Chem. Res.* **2013**, *46*, 1053−1061.
(53) Wang, C.; Zhang, H. R.; Li, J. D.; Chai, J. C.; Dong, S. M.; Cui, G. L. The interfacial evolution between polycarbonate-based polymer electrolyte and Li-metal anode. *J. Power Sources* **2018**, *397*, 157−161.
(54) Duan, H.; Fan, M.; Chen, W. P.; Li, J. Y.; Wang, P. F.; Wang, W. P.; Shi, J. L.; Yin, Y. X.; Wan, L. J.; Guo, Y. G. Extended Electrochemical Window of Solid Electrolytes via Heterogeneous Multilayered Structure for High-Voltage Lithium Metal Batteries. *Adv. Mater.* **2019**, *31*, No. 1807789.
(55) Choudhury, S.; Mangal, R.; Agrawal, A.; Archer, L. A. A Highly Reversible Room-Temperature Lithium Metal Battery Based on Crosslinked Hairy Nanoparticles. *Nat. Commun.* **2015**, *6*, 10101.
(56) Pang, X.; Zhao, L.; Han, W.; Xin, X.; Lin, Z. A General and Robust Strategy for the Synthesis of Nearly Monodisperse Colloidal Nanocrystals. *Nat. Nanotechnol.* **2013**, *8*, 426−431.
(57) Pang, X.; He, Y.; Jung, J.; Lin, Z. 1D Nanocrystals with Precisely Controlled Dimensions, Compositions, and Architectures. *Science* **2016**, *353*, 1268−1272.

https://doi.org/10.1021/acs.nanolett.1c02558
Nano Lett. 2021, 21, 7435−7447